*Witold Słówko, Andrzej Mulak**

Influence of the Spherical Aberration on the Current Density Distribution in the Electron Beam

In the paper a method of evaluation of the influence of the electronooptical aberration on the electron beam current density distribution is discussed. Assuming that the primary current density distribution is of the Gaussian type the current density distributions in the Gaussian image plane as well as in the best focus plane have been determined on the base of the postulated method including the influence of the spherical aberration. The considerations are illustrated by examples. Finally, the problem of magnification and aperture angle optimization have been discussed for the beam disturbed by the spherical aberration. The purpose of the optimization is to obtain the maximum current density on the axis.

1. Current Density Distribution in Perfect Imaging

In contemporary technology an increasing application of the electron beam as a working tool is being observed. The applicability of the electron beam to particular kinds of treatment is determined by its diameter in the working plane, the value and distribution of the current density in that plane and the electron beam energy.

In the electron beam machine the beam focussing in the working plane is realized by imaging the pupil of the electrono-optical gun (being the source of the electrons) onto this surface. The influence on the imaging errors including the spherical aberration can be observed in the form of enlarging of the beam diameter as well as changes in the current density distribution in the working plane as compared to the perfect imaging.

The basic parameter of the electron beam is the so called electron brightness. It is understood as a ration of the current density of a virtual electron source (electronooptical crossover) to the solid angle. In the differential form the electron brightness may be described by the formula [1]:

$$B = \frac{\partial^2 I}{\partial A \partial \omega}, \tag{1}$$

where I — electron beam current,

A — cross-section of the beam in the electronooptical crossover,

ω — solid angle subtended by the beam.

*) Institute of Electron Technology, Technical University of Wrocław, Wrocław, ul. Janiszewskiego 11/17, Poland.

In this formula the symbol of partial differentiation has been used though in the general case the current I is not a unique function of A and ω. The electron brightness defined in this way takes the same value for the corresponding elements of the object and the image in the case of aberration free imaging.

If the electron brightness for the given region is known, then the current density may also be determined within this region on the base of the formula

$$J = \frac{\partial I}{\partial A} = \int_0^{\omega} B d\omega. \tag{2}$$

In the case of the electron beams exhibiting the axial symmetry it is more convenient to use the aperture angle α and the azimuth φ instead of the solid angle ω. Then the element of the electron beam solid angle (see Fig. 1) may be described as

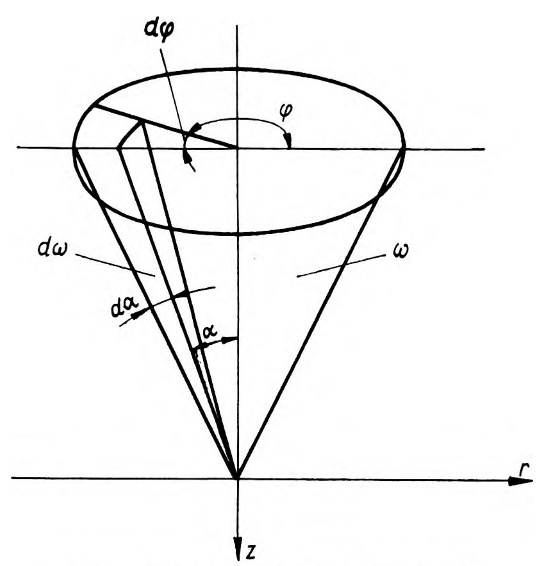

Fig. 1. Solid angle element of the beam

$$d\omega = a da d\varphi, \tag{3}$$

for the sufficiently small angle a.

If the aperture angle of the beam is small (for instance as a result of the applied diaphragm) it may be assumed that the electron brightness of the image point under discussion as well as that of the object points does not depend on the angles a and φ. Under these circumstances the expression (2) may be reduced to the form:

$$J \simeq \int_0^a \int_0^{2\pi} B a d\varphi da \simeq B\pi a^2. \tag{4}$$

In accordance with the calculation carried out by Langmuir the radial distribution of the current density in the electronooptical crossover is of a Gaussian type (see [2], [3]):

$$J_0\ (r) = J_0\ \exp\left(-\frac{r^2}{a_0^2}\right), \tag{5}$$

where J_0 denotes the current density of the crossover axis.

The above dependence has been derived under the following conditions:

a) electrons leave the cathode with the Maxwell velocity distribution,

b) sine Abbe's law is satisfied in the region of the cathod lens,

c) cathod lens is free from aberrations and the influence of the space charge may be neglected.

In the electron guns realized in practice the said assumptions are not met and the current density distribution may deviate from the Gaussian distribution, the latter being accepted as a basis for the discussion presented in this paper.

A comparison of the relations (4) and (5) allows to infer that the Gaussian distribution of the current density in the electronooptical crossover should correspond to the same distribution of the electron brightness:

$$B_0\ (r) = B_0\ \exp\left(-\frac{r^2}{a_0^2}\right), \tag{6}$$

where

$$B_0 = \frac{J_0}{\pi a_0^2},$$

and a_0 is the aperture angle of the beam in the electronooptical crossover.

In the case of perfect imaging of the electronooptical crossover with the linear magnification M the value of the aperture angle and the constant a (the latter being a scale factor for the coordinate r) will be changed accordingly. If the imaging system fulfils the condition of the inverse proportionality of the angular and linear magnifications then the current density distribution $J_1(r)$ as well as the brightness distribution $B_1(r)$ in the image are given by the formulae

$$B_1(r) = B_0\ \exp\left(-\frac{r^2}{a_1^2}\right), \tag{7}$$

$$J_1(r) = \pi B_1(r) \alpha_1^2 \tag{8}$$

respectively, where $a_1 = \frac{a_0}{M}$, $a_1 = a_0 M$.

Hence an expression for the maximum beam current density in the image plane is obtained in the form

$$J_1 = \frac{\pi B_0 a_0^2}{M^2} = \frac{J_0}{M^2}. \tag{9}$$

On the base of this it can be concluded, that in the case of perfect imaging arbitrary great values of the beam current density may be obtained providing that the respectively high demagnification of the imaging system can be realized.

2. Influence of the Spherical Aberration on the Beam Current Density Distribution in the Gaussian Image Plane

The influence of the spherical aberration on the current density distribution of the beam in the imaging plane was considered by Küchne [4]. He also assumed that the beam current density distribution without spherical aberration has the form of the Gaussian distribution. By differentiating the distribution and taking into account the current spread within each interval by the amount equal to the diffusion circle Δ_{sph} the author obtained the real distribution as an arythmetic average of the average current densities of the neighbouring intervals. This procedure is very tedious and does not assure sufficient accuracy.

For considering the influence of the imaging errors on the density distribution another method may be proposed, in which the problem is treated more generally and with greater accuracy.

The electron beam current reaching the arbitrary point in the image is a sum of the elementary current streams contained in the infinitesimally small solid angles $d\omega$. The current density of the elementary current stream is given by the expression

$$dJ = Bd\omega = B a d a d\varphi, \tag{10}$$

in accordance with the relations (2) and (3). All the current streams energing from an object point and contained within the angle limits $0 \leqslant \alpha \leqslant \alpha_1$ and $0 \leqslant \varphi \leqslant 2\pi$ reach the ideal image point of the coordinate ϱ. Hence the current density at this point is defined by the relationship

$$J_1(\varrho) = \int\limits_0^{\alpha_1}\int\limits_0^{2\pi} B_1(\varrho)\,\alpha\, d\varphi\, d\alpha = \int\limits_0^{\alpha_1}\int\limits_0^{2\pi} B_0 \times \tag{11}$$

$$\times \exp\left(-\frac{\varrho^2}{a_1^2}\right)\alpha\, d\varphi\, d\alpha.$$

If the spherical aberration appears, the same real image point of the coordinate r is fed by the elementary streams, which in the case of perfect imaging would be directed to various points in the image of different coordinates ϱ. These points are contained within the circle of radius $\Delta(\alpha_1)$ determined by the spreading due to the spherical aberration as it is shown diagramatically in Fig. 2. Hence, it follows

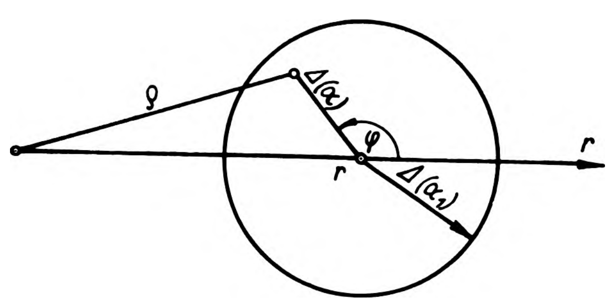

Fig. 2. Region, from which the current streams are delivered to the point of the coordinate r

that the coordinate ϱ of the primary (ideal) image point transferring one of the current streams to the real image point of the coordinate r is a function of r and $\Delta(\alpha)$ as well as of the angle φ. From the Carnot formula we obtain the following dependence of the coordinate ϱ on the said quantities

$$\varrho^2 = r^2 + \Delta^2(\alpha) + 2\Delta(\alpha) r \cos\varphi. \tag{12}$$

After substituting the above relations into the formula (11) the expression describing the current density at an arbitrary point of the coordinate r in the real image takes the following form:

$$J_{1_s}(r) = \int\limits_0^{\alpha_1}\int\limits_0^{2\pi} B(r, \alpha, \varphi)\,\alpha\, d\varphi\, d\alpha \tag{13}$$

$$= \int\limits_0^{\alpha_1}\int\limits_0^{2\pi} B_0 \exp\Bigg[-\frac{1}{a_1^2}\left(r^2 + \Delta^2(\alpha) + \right.$$

$$\left. + 2\Delta(\alpha) r \cos\varphi\right)\Bigg]\alpha\, d\varphi\, d\alpha.$$

If only the spherical aberration occurs the error $\Delta = \Delta(\alpha)$ does not depend on the azimuthal coordinate φ and the above formula may be written in another way

$$J_{1_s}(r) = B_0 \exp\left(-\frac{r^2}{a_1^2}\right) \times \tag{14}$$

$$\times \int\limits_0^{\alpha_1}\left[\exp\left(-\frac{\Delta^2}{a_1^2}\right)\int\limits_0^{2\pi} \exp\left(-\frac{2r\Delta\cos\varphi}{a_1^2}\right) d\varphi\right]\alpha\, d\alpha.$$

Integrating over the variable φ gives the following result [6]:

$$\int\limits_0^{2\pi} \exp\left(-\frac{2r\Delta\cos\varphi}{a_1^2}\right) d\varphi = 2\pi I_0\left(\frac{2r\Delta}{a_1^2}\right), \tag{15}$$

where I_0 is the modified Bessel function of the first kind and zeroth order.

To perform further the integration the expression on the right hand side of (15) should be expanded into series

$$2\pi I_0\left(\frac{2r\Delta}{a_1^2}\right) = 2\pi\left(1 + \frac{r^2\Delta^2}{a_1^4} + \frac{r^4\Delta^4}{4a_1^8} + \ldots\right). \tag{16}$$

For the same reason also the function $\exp\left(-\frac{\Delta^2}{a_1^2}\right)$ is most conveniently represented in a similar form

$$\exp\left(-\frac{\Delta^2}{a_1^2}\right) = 1 - \frac{\Delta^2}{a^2} + \frac{\Delta^4}{2a_1^4} - \ldots \tag{17}$$

If the accuracy resulting from truncation of the series after the third term is satisfactory the dependence (14) may be represented in the following form

$$J_{1_s}(r) = 2\pi B_0 \exp\left(-\frac{r^2}{a_1^2}\right) \times \tag{18}$$

$$\times \int\limits_0^{\alpha_1}\Bigg[1 + \frac{\Delta^2}{a_1^2}\left(\frac{r^2}{a_1^2} - 1\right) + \frac{\Delta^4}{a_1^4}\left(\frac{r^4}{4a_1^4} - \frac{r^2}{a_1^2} + \frac{1}{2}\right) +$$

$$+ \frac{\Delta^6}{a_1^8}\left(\frac{1}{2} - \frac{r^2}{4a^2}\right) r^2\Bigg]\alpha\, d\alpha.$$

As the spherical aberration error in the Gaussian image plane is determined by the relationship

$$\Delta = \Delta_{\mathrm{sph}} = C_s^* \alpha^3, \tag{19}$$

where C_s^* is the modified constant of the spherical aberration [5] the expression (17) — after having been integrated — generates the following formula describing the current density distribution of the beam in that plane:

$$J_{1_s}(r) = 2\pi B_0 \exp\left(-\frac{r^2}{a_1^2}\right)\left[\frac{\alpha_1^2}{2} + \frac{1}{8a_1^2} \times \right.$$

$$\times \left(\frac{r^2}{a_1^2} - 1\right) C_s^{*2} \alpha_1^8 + \frac{1}{14a_1^4}\left(\frac{r^4}{4a_1^4} - \frac{r^2}{a_1^2} + \frac{1}{2}\right) \times$$

$$\left. \times C_s^{*4} \alpha_1^{14} + \frac{r^2}{40a_1^8}\left(1 - \frac{r^2}{2a_1^2}\right) C_s^{*6} \alpha_1^{20}\right]. \quad (20)$$

3. Current Density Distribution of the Beam in the Plane of Best Focussing

In the electron beam machine the working surface is not identical with the Gaussian image plane and should be located in the place where the diameter of the aberrated beam is the smallest.

If the error due to spherical aberration is small its value in the analyzed plane located at a distance z from the Gaussian image plane may be described by the formula:

$$\Delta_z' = C_s^* \alpha^3 + \alpha z. \quad (21)$$

When substituting this error equation (21) to the relation (18) the following formula for the current density distribution in the plane z results

$$J_{1_s}(r, z) = 2\pi B_0 \exp\left(-\frac{r^2}{a_1^2}\right)\left[\frac{\alpha_1^2}{2} + \left(\frac{r^2}{a_1^2} - 1\right) \times \right.$$

$$\times \left(\frac{\alpha_1^4}{4} z^2 + \frac{\alpha_1^6}{6} 2C_s^* z + \frac{\alpha_1^8}{8} C_s^{*2}\right)\frac{1}{a_1^2} + \frac{1}{a_1^4}\left(\frac{r^4}{4a_1^4} + \frac{-r^2}{a_1^2} + \right.$$

$$\left. + \frac{1}{2}\right)\left(\frac{\alpha_1^6}{6} z^4 + \frac{\alpha_1^8}{8} 4C_s^* z^3 + \frac{\alpha_1^{10}}{10} 6C_s^{*2} z^2 + \frac{\alpha_1^{12}}{12} 4C_s^{*3} z + \right.$$

$$\left. + \frac{\alpha_1^{14}}{14} C_s^{*4}\right) + \frac{r^2}{a_1^8}\left(\frac{1}{2} - \frac{r^2}{4a_1^2}\right)\left(\frac{\alpha_1^8}{8} z^6 + \frac{\alpha_1^{10}}{10} 6C_s^* z^5 + \right.$$

$$+ \frac{\alpha_1^{12}}{12} 15C_s^{*2} z^4 + \frac{\alpha_1^{14}}{14} 20C_s^{*3} z^3 + \frac{\alpha_1^{18}}{18} 6C_s^{*5} z +$$

$$\left. \left. + \frac{\alpha_1^{20}}{20} C_s^{*6}\right)\right]. \quad (22)$$

To determine the coordinate z for the best beam focussing plane the theory of caustic may be used. In Fig. 3 the process of spherical aberration error formation has been shown diagramatically for the case of point imaging. The shape of the diacaustic surface, being a locus of the intersection points of the neighbouring electron trajectories, is marked

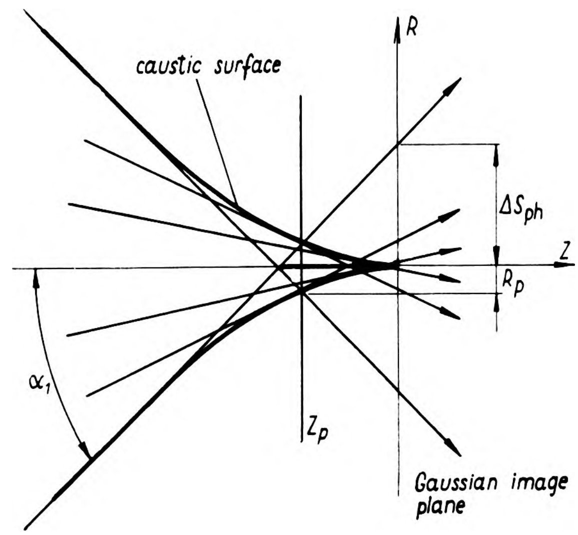

Fig. 3. Schematic mechanism of spherical aberration error creation

there as well. In the case when only the spherical aberration occurs the equation of the last surface may be represented in the following form

$$R = -\alpha z + C_s^* \alpha^3,$$
$$z = -2C_s^* \alpha^2 \pm C_s^* \alpha^2. \quad (23)$$

In only the external causting surface is taken into consideration we get

$$R = -2C_s^*\left(\frac{-z}{3C^*}\right)^{3/2} \quad (24)$$

after having eliminated α.

The beam narrowing occurs in the place of intersection of the external electron beams travelling under the angle α_1 with the caustic i.e. in the plane $z = z_p$. Thus in this plane the expressions (21) and (24) may be compared to each other i.e.

$$\alpha_1 z_p + C_s^* \alpha_1^3 = -2C_s^*\left(\frac{-z_p}{3C_s^*}\right)^{3/2}. \quad (25)$$

The minus sign on the right hand side denotes that the intersection is realized by the rays, which travel on the side opposite to that of the rays creating the caustic at the intersection points. The solving of the above equation results in determination of the coordinate of the best focus plane

$$z_p = -\frac{3}{4} C_s^* \alpha_1^2. \quad (26)$$

The radius of the beam cross section being

$$R_p = \frac{1}{4} C_s^* \alpha_1^3 \quad (27)$$

is four times smaller than that of the confusion circle due to the spherical aberration at the Gaussian image plane.

After substituting $z = z_p$ to the formula (22) and certain rearrangements the following expression for the current density in the best focus plane is obtained

$$
\begin{aligned}
J_{1s}(r, z_p) = J_1(r) \Bigg[1 + \left(\frac{r^2}{a_1^2} - 1\right) \frac{3.12 \cdot 10^{-2} \Delta_{\text{sph}}^2}{a_1^2} + \\
+ \left(\frac{r^4}{4a_1^4} - \frac{r^2}{a_1^2} + \frac{1}{2}\right) \frac{1.4 \cdot 10^{-3} \Delta_{\text{sph}}^4}{a_1^4} + \\
+ \frac{r^2}{a_1^2} \left(\frac{1}{2} - \frac{r^2}{4a_1^2}\right) \frac{2 \cdot 10^{-4} \Delta_{\text{sph}}^6}{a_1^6} \Bigg],
\end{aligned} \tag{28}
$$

where Δ_{sph} denotes the error of the spherical aberration in the Gaussian plane, while $J_1(r)$ is an aberration—free current density distribution in the same plane. The current density distribution including the spherical aberration in the Gaussian plane may be represented in a similar form

$$
\begin{aligned}
J_{1s}(r, 0) = J_1(0) \Bigg[1 + \left(\frac{r^2}{a_1^2} - 1\right) \frac{0.25 \Delta_{\text{sph}}^2}{a_1^2} + \\
+ \left(\frac{r^4}{4a_1^4} - \frac{r^2}{a_1^2} + \frac{1}{2}\right) \frac{0.143 \Delta_{\text{sph}}^4}{a_1^4} + \frac{r^2}{a_1^2} \left(\frac{1}{2} - \frac{r^2}{4a_1^2}\right) \times \\
\times \frac{0.05 \Delta_{\text{sph}}^6}{a_1^6} \Bigg].
\end{aligned} \tag{29}
$$

When comparing both relations it is clear that the current density distributions in the Gaussian plane and the plane of best focus are of different type. Independently, it should be reminded that the above formulae may be considered to be of sufficient accuracy only for small values of the relative errors Δ_{sph}/a_1 and small radia r/a_1 (because only three terms of the expansion were taken into further consideration). Calculations for the arbitrarily wide range of a may be performed by numerical integrating of expression (14).

As an example the current density distribution of a beam in the Gaussian plane and in the best focus plane has been calculated in the presence of spherical aberration. The results of computing in the reduced coordinates are presented in the form of graphs in Fig. 4.

The values of the current density in the graphs on the left hand side of the Figure are plotted as referring to the maximal value of each curve, while those on the right hand size of the Figure refer to the maximal value of the corresponding (primary) aberration--free distributions. The curve a presents a Gaussian (aberration-free) current density distribution. The curves b and c correspond to the current density distribution in both the Gaussian image plane and the best focus plane and are calculated from the formulae (28) and (29), respectively, under the assumption of a relatively great error of spherical aberration $\Delta_{\text{sph}} = a_1$, ($C_s^* = 10^3 a_1$, $a_1 = 0.1$). On the other hand the curves d and e represent similar distributions taking account the spherical aberration error of even

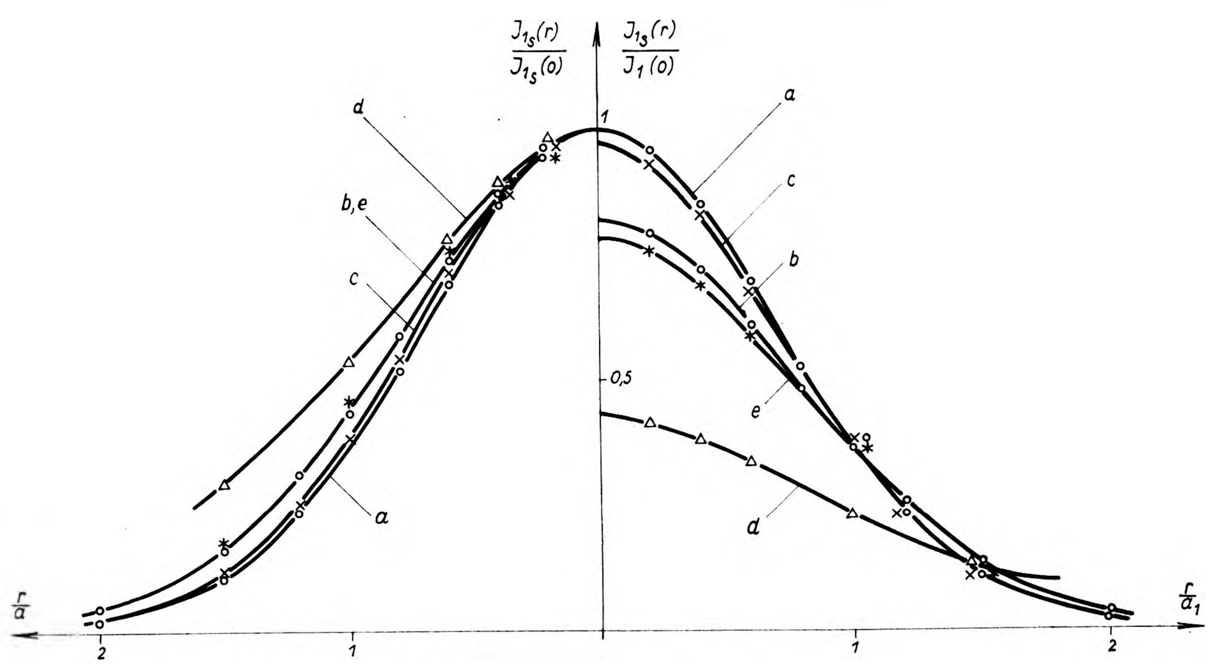

Fig. 4. Current density distributions of the beam

a— $a_1 = 0.1$; $C_s^* = 0$ ($\Delta_{\text{sph}} = 0$); $z = 0$. b— $a_1 = 0.1$; $C_s^* = 10^3 a_1$ ($\Delta_{\text{sph}} = a_1$); $z = 0$.
c— $a_1 = 0.1$; $C_s^* = 10^3 a_1$ ($\Delta_{\text{sph}} = a_1$); $z = z_p$. d— $a_1 = 0.1\sqrt{2}$; $C_s^* = 10^3 a_1$ ($\Delta_{\text{sph}} = 2\sqrt{2} a_1$); $z = 0$.
e— $a_1 = 0.1\sqrt{2}$; $C_s^* = 10^3 a_1$ ($\Delta_{\text{sph}} = 2\sqrt{2} a_1$); $z = z_p$

greater value of $\Delta_{\text{sph}} = 2\sqrt{2}a_1$, ($C_s^* = 10^3 a_1$, $a_1 = 0.1\sqrt{2}$). In this case the calculations have been performed by way of numerical integrating of the relation (14) and using the method of rectangulers. In the course of integration the intervals of integrating have been devided into fifteen subregions and the values of the function in the midpoint of each subinterval have been accepted. From the presented graphs it may be concluded, that the influence of the spherical aberration on the current density distribution of the beam is mainly displayed by the decrease of the latter in the vicinity of the beam axis and its increase in the external zone. The half-width of the distribution curve is changed slightly at the same time. Also these calculations confirm the thesis that the current density distribution is much more advantageous in the best focus plane than in the Gaussian image plane.

4. Optimizing the Magnification and the Aperture Angle of the Beam

The degree of deformation of the current density distribution is the beam in the working plane and the respective diminishing of the current density as compared to the primary distribution depends on the magnitude of the spherical aberration error and, by the same means, on both the spherical aberration constant C_s^* and the beam aperture angle α_1. To reduce this error the most convenient way would be to deminish the value of the spherical aberration constant. However, practical possibilities of performing such an operation are limited. The spherical aberration error may be arbitrarily reduced by way of the corresponding reduction of the beam aperture angle α_1. Howevr, this results in the current density loweringe in the eprimary distribution. An achievement of th maximum beam current density in the presence of the spherical aberration requires the beam aperture angle to be selected optimally. This optimizing may be done on the base of the following simplified model taken as a first approximation. Namely, it may be assumed that the electronooptical crossover — being the subject of imaging — is of finite diameter d_0, while the electron brightness B_0 is constant within its region. The current density in the ideal pupil image of diameter d_1 is given by relation (9). The influence of the spherical aberration on the current density may be included by assuming that the spherical aberration error measured in the plane of best focus is additive with respect to the primary diameter and thus causes a dimishing of the current densitv in accordance with the relation

$$J_{1s} = J_1 \left(\frac{d_1}{d_1 + d_s}\right)^2, \tag{30}$$

where,

$$d_s = 2R_p = \frac{1}{2} C_s^* \alpha_1^3. \tag{31}$$

The optimal selection of the beam aperture angle may be done in two ways: by introducing an aperture diaphragm or — in the systems without diaphragms — by matching the magnification.

In the last case dependence (31) may be put in the form,

$$J_{1s} = \frac{B_0 \pi \alpha_0^2}{M^2} \left(\frac{M d_0}{M d_0 + \frac{C_s^{*3} \alpha_0}{2M^2}} \right)^2. \tag{32}$$

By differentiating the relation and comparing the result to zero the optimum value of the linear magnification M_{opt} which generates the maximal beam current density in the sample plane, may be determined.

$$M_{\text{opt}} = \frac{3 d_s}{d_0}. \tag{33}$$

Hence

$$d_s = \frac{1}{3} d_1.$$

The determination of the optimal aperture angle by done by a similar method, when using expressions (30) and (31) for the current density in the working plane. The magnification is then defined by the assumed beam diameter $d_1 = M d_0$. As a result the following expression for the optimum magnitude of the beam aperture angle α_1 is obtained

$$\alpha_{1\text{opt}} = \left(\frac{d_1}{C_s^*}\right)^{1/3}, \tag{34}$$

where $d_1 = 2d_s$ or, when assuming that the entire beam diameter in the working surface is equal to

$$d_c = d_1 + d_s \tag{35}$$

we get

$$\alpha_{1\text{opt}} = \left(\frac{2}{3} \frac{d_c}{C_s^*}\right)^{1/3}. \tag{36}$$

The last form of the expression for the optimal value of the aperture angle is often cited in literature devoted to the electron beam machine [7, 8, 9].

The optimal magnification magnitude as well as that of the aperture angle may be determined with considerably better accuracy, when assuming the Gaussian distribution of the current density and basing on the relations derived earlier and describing the influence of the spherical aberration. If it is assumed that the purpose of optimizing is in generating the greatest possible current density on the beam axis i.e. for $r = 0$ then on the base of expression (14) the value of the current density at this point appears as given in the form

$$J_{1s}(0) = 2\pi B_0 \int_0^{a1} \exp\left(-\frac{\Delta^2}{a_1^2}\right) a\,da. \tag{37}$$

When taking two terms of expansion (17) and repeating the procedure described earlier the following expression for the current density on the axis in the best focus plane is obtained

$$J_{1s}(0,z_p) = 2\pi B_0 \left(\frac{\alpha_1^2}{2} - \frac{C_s^{*2}\,\alpha_1^8}{a_1^2 \cdot 64}\right). \tag{38}$$

If an account is taken of the fact that $\alpha_0 = M\alpha_1$ and $a_1 = Ma_0$ the optimum magnification magnitude is expressed by the formula

$$M_{\mathrm{opt}} = \sqrt[8]{\frac{C_s^{*2}\,\alpha_0^6}{6.4a_0^2}} \tag{39}$$

obtained by differentiating (38) and equaling the result to zero.

After some further transformations it may be shown that the optimum value of the magnification is also given by the condition

$$M_{\mathrm{opt}} = \frac{d_s}{1.17a_0} \tag{40}$$

which may be put in the form

$$d_s = 1.17a_1. \tag{41}$$

It is convenient to assume that the beam diameter is equal to the width of the current density distribution curve understood as the distance between the points at which the current density drops to $1/e$ of its maximal value. Then

$$d_1 = 2a_1. \tag{42}$$

In the case of application of the aperture diaphragm the optimal aperture angle magnitude evaluated (similarly to the former cases) from the formula (38) is represented by the formula

$$\alpha_{1\,\mathrm{opt}} = \sqrt{2}\left(\frac{a_1}{C_s^*}\right)^{1/3} \tag{43}$$

which corresponds to the condition

$$d_s = \sqrt{2}a_1, \text{ or } \Delta_{\mathrm{sph}} = 2\sqrt{2}a_1. \tag{44}$$

A comparison of the above results with those yielded by the simplified analysis in the form of (33) and (34) evidences, that under the condition of optimal magnification or optimal aperture angle selection, much greater values for the spherical aberration error are allowed than those established earlier. The value of the maximum current density obtained in this way is also much greater.

If we assume that on the beam axis the electron brightness in the electronooptical crossover is equal to the maximal theoretical value given by Langmuir

$$B_{0t} = \frac{J_k U_0}{\pi U_T}, \tag{45}$$

where J_k — cathod current density, U_T — electrokinetic potential und U_0 — accelerating voltage then the maximum current density in the best focus plane for optimal aperture angle is given by

$$J_{1\max}(0) \simeq 1.5J_k \frac{U_0}{U_T}\left(\frac{a_1}{C_s^*}\right)^{2/3} \tag{46}$$

in accordance with (38) and (43). In practice, the electron brightness ranges between 4–90% of its theoretical value and the expected value of the current density should be also less by the same amount.

The maximal value of the current density for the beam blurred by the spherical aberration is, as may be easily appreciated, equal to 75% of the aberration-free beam current density of the same aperture angle. Because of truncation of the series (17) on the second term the said value is slightly lowered. When the three terms are included the value is raised up to as high as 80% of the ideal beam current density, which is however too optimistic. Finally, by way of numerical integrating of formula (14) it has been estimated that the current density on the beam axis of optimal aperture angle amounts to 78.2% of the aberration-free beam current density. The optimal current density distribution in the beam is illustrated by the curves in Fig. 4.

5. Concluding Remarks

In the paper an analysis of the influence of the spherical aberration on the current density distribution in the electron beam is given under the assumption that the primary distribution in the beam is of the Gaussian type. The results obtained are a basis of the analysis aiming at the optimalization of the beam parameters important in the micro-working process.

It seems to be worth emphasizing that the analysis may be generalized in two respects: as far as the primary current density distribution in the beam is concerned and by changing the kind of the electronooptical aberration. For the purpose a corresponding function of the primary distribution $B = B(r, \alpha, \varphi)$ has to be introduced to formula (13) and a dependence characterizing the kind of aberration should be treated in the place of (19). These changes in the primary distribution as well as the kind of aberration alter the conditions for obtaining the beam of optimal parameters.

L'influence de l'aberration sphérique sur la repartition de la densité du courant d'un faisceau électronique

Dans cet article on a présenté une méthode qui tient compte de l'influence des aberrations électro-optiques sur la repartition de la densité du courant d'un faisceau électronique. En admettant que la repartition primitive de la densité de courant du faisceau est une repartition de Gauss, on a déterminé, à l'aide de cette méthode, les repartitions de la densité de courant dans l'espace de l'image gaussienne et dans l'espace de la focalisation optimale, en tenant compte de l'influence de l'aberration sphérique. Le tout a été illustré avec des exemples. En conclusion on a traité le problème de l'optimisation de l'agrandissement et de l'angle d'ouverture du faisceau déformé par l'aberration sphérique. L'optimisation a pour but l'obtention de la densité maximale de courant sur l'axe du faisceau.

Влияние сферической аберрации на распределение плотности тока электронного пучка

В статье обсужден метод учета влияния электронно-оптических аберраций на распределение плотности тока электронного пучка. На основе предположения о том, что первоначальное распределение плотности тока пучка представляет собой гауссово распределение, определили, по предлагаемому методу, распределения плотности тока в гауссовой плоскости изображения и в плоскости оптимальной фокусировки, учитывающие влияние сферической аберрации. Обсуждение проиллюстрировано примерами. В заключении рассмотрен вопрос об оптимизации увеличения и апертурного угла пучка, деформированного сферической аберрацией. Цель оптимизации заключается в получении максимальной плотности тока на оси пучка.

References

[1] Hanszen K., Lauer R., *Richtstrahlwertmessungen mit dem Zwei-Blendenverfahren an Elektronenstrahlen mit Kugelkatoden von 250 bis 1,5 μm Durchmesser*, Z. Naturforschg.., t. 22a, p. 238 (1967).

[2] Moss H., *The electron gun of the catode ray tube*, Part 1 — J. Brit. J. R. E., January 1945, Part 2 — J. Brit. J. R. E., May 1946.

[3] Friedel K., Hałas A., *Pomiar parametrów wiązki elektronowej w obszarze soczewki katodowej stosowanej w kineskopie AW-47-91*, Prace Naukowe I. T. E. Politechniki Wrocławskiej, No. 4, Studia i Materiały No. 3/197.

[4] Küchne W., *Zum Einfluss des Öffnungsfehlers bei Strahlbearbeitungsgeräten*, Third Czechoslovak Conference on Electronics and Vacuum Physics Transactions, Praha 1965.

[5] Słówko W., *Parametry elektronooptyczne zwierciadła dwururowego*, Prace Naukowe I.T.W. Politechniki Wrocławskiej. No. 6, Studia i Materiały. No. 5, p. 89 (1972).

[6] Ryżyk I. M., Gradsztejn I. S., Tablice całek, sum, szeregów i iloczynów, PWN, Warszawa 1964.

[7] Einstein P. A., Harvey D. R., Simmons P. J., *The design of an experimental electron beam machine*, Journal of Scientific Instr., **40**, 562 (1963).

[8] Vaucher J. G., et al., *Design and control of a high-precision electron beam machine*, The Radio and Electronic Engineer, Febr. 1967, p. 83.

[9] Szymański H., Friedel K., Słówko W., Mikroobróbka wiązką elektronową, WNT, Warszawa 1972.

Received, January 3, 1973